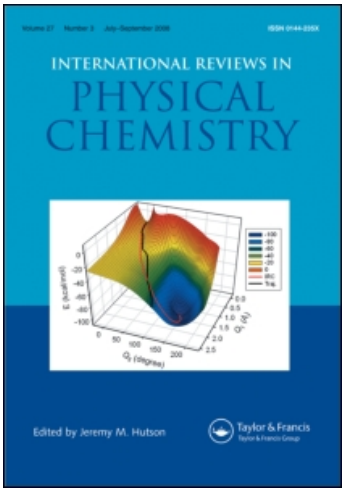


**International Reviews in Physical Chemistry**
Publication details, including instructions for authors and subscription information:
http://www.informaworld.com/smpp/title~content=t713724383

# Electronic excitation transport in disordered infinite volume systems

M. D. Ediger[a]; M. D. Fayer[a]
[a] Department of Chemistry, Stanford University, Stanford, California, USA

**To cite this Article** Ediger, M. D. and Fayer, M. D.(1985) 'Electronic excitation transport in disordered infinite volume systems', International Reviews in Physical Chemistry, 4: 3, 207 — 235
**To link to this Article: DOI:** 10.1080/01442358509353360
**URL:** http://dx.doi.org/10.1080/01442358509353360

INTERNATIONAL REVIEWS IN PHYSICAL CHEMISTRY, 1985, VOL. 4, NO. 3, 207–235

# Electronic excitation transport in disordered infinite volume systems

by M. D. EDIGER and M. D. FAYER
Department of Chemistry,
Stanford University, Stanford, California 94305, U.S.A.

An account of recent theoretical and experimental advances in the field of excitation transport in disordered systems is presented. First the problem of excitation transport among chromophores (donors) randomly distributed in solution is discussed. Picosecond fluorescence mixing experiments demonstrate that the recent nonperturbative theory for this type of system is accurate at all times and concentrations examined. Next we consider systems with two types of chromophores, donors and traps, randomly distributed in solution. Experiments and theory describe the transport and trapping of excitations over the full range of donor and trap concentrations. These ideas and picosecond transient grating experiments are used to explain the mechanism for fluorescence quenching in concentrated dye solutions, which is shown to be due to excitation transport and trapping by dimers of dye molecules. Finally, the problems of excitation transfer among molecules randomly distributed on a lattice (rather than in a solution) is discussed. An accurate nonperturbative theory is employed to calculate transport observables.



## 1. Introduction

During the past four years, rapid advances have been made in both our theoretical and experimental understanding of the transport of electronic excitations among molecules which are not in regular arrays. The transport of electronic excitations has been studied extensively in a wide variety of molecular materials: mixed crystals (Gentry and Kopelman 1983, Gentry 1983, Kopelman 1981, Smith *et al.* 1977, Colson *et al.* 1977), amorphous solids (Klafter and Jortner 1977), liquids (Gochanour and Fayer 1981, Miller *et al.* 1983, Millar *et al.* 1981, Rehm and Eisenthal 1971, Porter and Tredwell 1978, Craver and Knox 1971, Hemenger and Perlstein 1973), micelles (Ediger *et al.* 1984, Kenney-Wallace *et al.* 1975, Koglin *et al.* 1981), polymers (Klöpffer 1981, Ng and Guillet 1982, Frank *et al.* 1980, Anderson *et al.* 1980, Gelles and Frank 1982) and biological systems such as the photosynthetic unit (Pearlstein 1964, Markvart 1978, Porter 1978, Moog *et al.* 1984).

Excitation transfer is caused by interactions between resonant energy levels on different molecules, one of which is in an electronic excited state (Förster 1948). These interactions can cause the excitation to 'hop' from the originally excited molecule to another molecule, without photon emission. The interaction energy, and hence the excitation transfer rate, decreases rapidly as the molecules get farther apart. Even so, excitation transport between molecules can be significant for intermolecular separations greater than 100 Å.

Current research in excitation transport focuses on using the well understood pairwise interactions of chromophores to describe the dynamics of systems with many interacting molecules. The bulk of theoretical and detailed experimental work has been directed toward pure crystals since the symmetry properties of the crystal lattice provide considerable aid in reducing the difficulties associated with the many-body

problem (Davydov 1971, Burland *et al.* 1977 a, b, Kenkre and Knox 1974 a, b, Grover and Silbey 1970, 1971). In materials other than pure crystals, the molecules of interest are solutes in some type of a solid or liquid solution where the major component, i.e., the host species, does not directly participate in the transfer process. In solutions, the molecules have a distribution of intermolecular distances and since the intermolecular interactions responsible for excited-state transport are distance dependent (Förster 1948), a distribution of transfer rates and pathways exists.

The distribution of transfer rates and pathways which exist in a disordered system makes a theoretical description of the excitation dynamics difficult. However, rigorous theoretical and experimental investigation of such systems yields insights into the fundamental nature of their dynamics. In addition, detailed understanding of excitation transport provides a method for determining the spatial configuration (Ediger *et al.* 1984, Ediger and Fayer 1983) or other properties of the chromophores in a system (Moog *et al.* 1984).

In this article a number of systems which have been studied recently will be discussed from a theoretical and experimental perspective. The systems discussed here are all large enough to be taken as infinite in extent. However, there are a variety of interesting systems in which chromophores are contained in a volume sufficiently small that energy transport properties are significantly affected by the limited size of the system. Such finite volume systems include isolated polymer coils containing chromophores, small aggregates of coils in polymer blends, micelles containing dye molecules, and photosynthetic units. A recent review article discusses progress in the study of excitation transport in these systems (Ediger and Fayer 1984).

The nature of excitation transport among chromophores (donors) distributed randomly in solution (Gochanour *et al.* 1979) is addressed in Section 3. This is a classic problem treated by Förster (1948) over 30 years ago. Förster simplified the complex problem of the disordered system by taking the donors to be equally spaced at the average spacing for a given donor concentration. Excitation transport within this approximation was shown to be diffusive, i.e., the mean-square-displacement of the excitation increases linearly in time. However, work in the last few years has shown that this is not an accurate description of excitation transport dynamics. Transport is not diffusive (Gochanour *et al.* 1979, Haan and Zwanzig 1978). Picosecond fluorescence mixing experiments (Gochanour and Fayer 1981) on rhodamine 6G in solution demonstrate that recent theoretical advances provide an accurate and comprehensive description of excitation transport among randomly distributed donors in an infinite solution. The new theory employs a diagrammatic approach to the solution of the master equation for this problem (Gochanour *et al.* 1979). This approach is very powerful and has been extended to other problems (Loring *et al.* 1982 a, b, 1983 a, b, 1984 a, b, Parson 1983, Frederickson *et al.* 1983 a, b, 1984).

Transport and trapping are then considered. The transport of electronic excitations in solutions containing traps was also addressed by Förster (1949). Trapping of electronic excitations is responsible for phenomena such as sensitized luminescence in crystals and solutions (Dexter 1953) and sensitized photochemistry such as photosynthesis (Pearlstein 1964, Markvart 1978, Porter 1978). The study of transport and trapping dynamics has become an important tool for investigating biological (Haas *et al.* 1975, Dale and Eisinger 1976) and polymer systems (Klöpffer 1981, Frank *et al.* 1980). Förster considered solutions containing two solute species: donor molecules and traps. An electronic excitation could be transferred from donor to trap via a resonant dipole–dipole interaction. (Subsequently the work was extended to

higher multipole and exchange interactions (Dexter 1953, Inokuti and Hirayama 1965)). Förster treated the case in which the trap concentration is much greater than the donor concentration. Each donor is assumed to interact only with an ensemble of neighbouring traps, so transport from one donor to another is neglected. Neglect of donor–donor transport greatly simplifies the theoretical problem.

By applying the diagrammatic technique developed for the donor–donor transport problem to donor–trap systems, it has been possible to obtain an accurate description of excitation transport dynamics for any concentration of donors and traps (Loring *et al.* 1982 a, b). Picosecond fluorescence mixing and transient grating experiments were employed to examine transport and trapping in solutions with a wide range of donor and trap concentrations (Miller *et al.* 1983). Comparisons of experiment and theory demonstrate that we have a comprehensive understanding of this type of system. (The general problem of donor–donor transport prior to trapping can be handled for any form of the intermolecular interaction distance dependence. While electronic excitations are being discussed here, the theoretical results apply to electron transport as well.)

In section 4, our understanding of transport and trapping in solution is applied to the problem of fluorescence quenching in concentrated dye solutions. Picosecond transient grating experiments were performed on concentrated solutions of rhodamine 6G (Lutz *et al.* 1981, Fayer 1982). It is shown that at high dye concentrations, three radiationless processes combine to quench fluorescence. They are donor–donor excitation transport, excitation trapping by dimers of dye molecules, and radiationless relaxation of the excited dimer. The onset of quenching with dye concentration is very rapid, having an approximately cubic dependence on concentration.

In Section 5, the random solution theory for transport and trapping of excitations is extended to the case of molecules randomly substituted on a lattice (Loring *et al.* 1983 a, b, 1984 a, b). In the lattice theory, the distance variable is no longer continuous. When performing ensemble averages over the possible positions of all particles, it is necessary to exclude configurations in which two molecules are on the same lattice site. This greatly increased the complexity of the problem. The diagrammatic theory for the lattice problem allows accurate results to be obtained from low concentration to a filled lattice. The theory can be used with any form of the transfer interaction and for any lattice type. The theory is compared to mixed crystal experiments (Gentry and Kopelman 1983, Gentry 1983) and found to be in good agreement.

The phenomenon of hopping transport in disordered systems is of considerable interest in many areas of solid state physics, chemistry, and biology. The net result of the work described in this series of articles is a greatly increased understanding of such processes and a strong foundation for further investigations.

## 2. Experimental methods

The picosecond experiments presented in the following sections are of two types: transient grating experiments, and fluorescence mixing experiments. These methods will be outlined in this sections.

The transient grating experiment (Lutz *et al.* 1981) is illustrated schematically in figure 1. Two time-coincident laser excitation pulses of wavelength $\lambda$ cross at an angle $\theta$ inside the sample, creating an interference pattern with fringe spacing $d$ given by $d=\frac{1}{2}\lambda \sin(\frac{1}{2}\theta)$. Optical absorption results in a spatially varying, sinusoidal excited-state concentration distribution. Since the optical properties of the excited states and ground states differ, the periodic excited-state concentration distribution acts as a transient

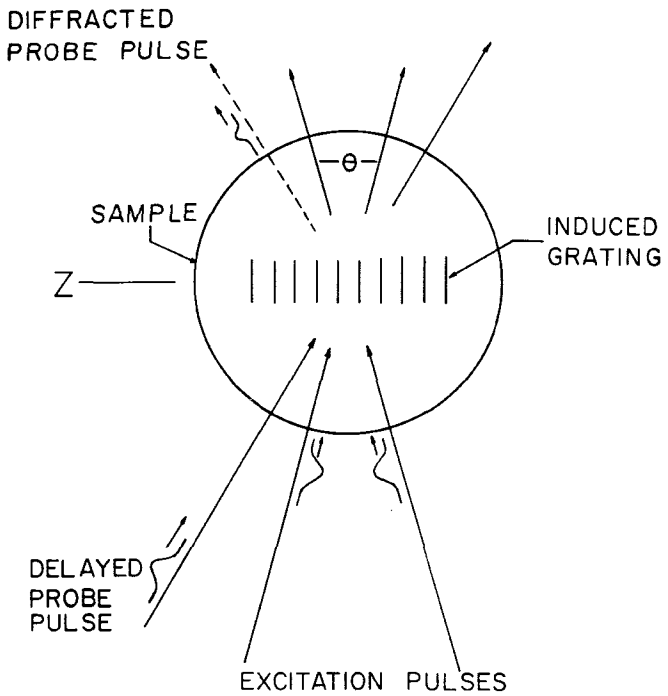


Figure 1. Schematic illustration of the transient grating experiment. Interference between the incoming excitation pulses results in an oscillatory density of excited states, which Bragg-diffracts the subsequent probe pulse. The diffracted probe, which reflects the time evolution of the excited state population, is the signal.



grating which diffracts a variably delayed probe laser pulse incident at the Bragg angle. The grating's diffracting power decays with time due to various excited-state dynamical processes. The time dependence is determined by measurement of the diffracted probe pulse intensity versus probe-pulse delay.

Transient grating (TG) experiments are used in our laboratory for several reasons. First, due to detection against a dark background, a TG experiment is inherently more sensitive than a probe pulse experiment. (In a probe-pulse experiment, a high-power pulse excites enough molecules into an excited state to change the absorption properties of the sample. A low-power probe pulse measures the absorption at various delay times after the initial excitation. The change in probe-pulse transmission with time yields the time dependence of the excited-state population.) In principle both experiments provide the same information about many processes of interest. Secondly, we found in probe-pulse experiments that highly concentrated samples required very large excitation power densities (small spot sizes) to achieve sufficient bleaching of the ground state population to give reasonable signal. These very high power densities resulted in anomalous power-dependent decays. In a TG experiment, because of its high sensitivity, large spot sizes can be used so the problem is avoided. In addition, the small fringe spacing associated with a TG experiment minimizes problems associated with reabsorption. Thirdly, there are a variety of measurements which can be made only by using transient grating approaches, e.g., exciton transport in pure crystals (Rose *et al.* 1984), phonon generation and detection (Fayer 1982, Nelson *et al.* 1982).

The transient grating experimental setup is illustrated in figure 2. The system as shown is arranged to perform experiments on high-concentration dye solutions which exhibit fluorescence quenching (Lutz *et al.* 1981) (Section 4). The laser is a continuously pumped Nd : YAG system which is acousto-optically Q-switched and mode-locked to produce trains of about 40 pulses at 1·06 $\mu$m with 1·3 mJ per pulse train. A single pulse is selected by a Pockels cell with an avalanche transistor driver and frequency tripled to yield a 10-$\mu$J, 50-ps pulse at 355 nm. This is split into the two excitation pulses which are recombined at the sample. The rest of the YAG pulse-train is separated by a reflecting polarizer, frequency doubled, and used to synchronously pump a dye laser which is spectrally narrowed and tuned by two intracavity etalons. The dye laser is cavity dumped using another Pockels cell with avalanche transistor driver to give a 20-$\mu$J, 30-ps pulse with a spectral width of 1 $cm^{-1}$. Both Pockels cells are triggered optically by

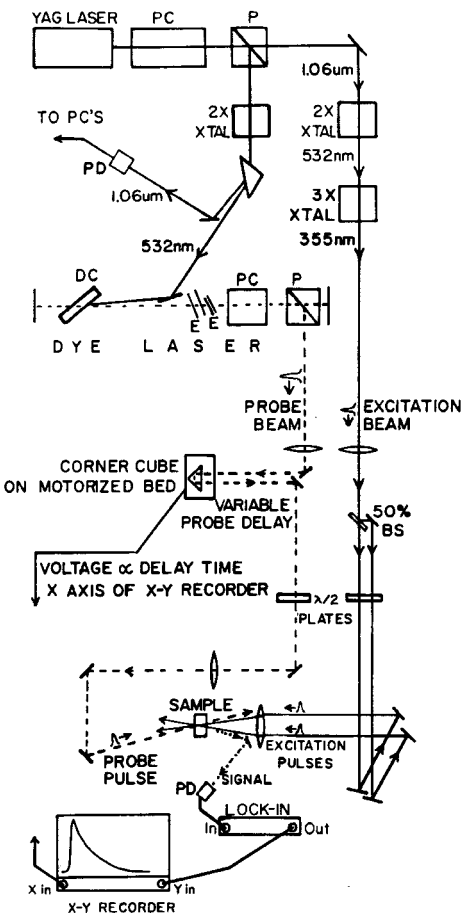


Figure 2. Transient grating experimental setup. A single 1·06 $\mu$m pulse is selected from the YAG mode-locked pulse train, frequency tripled to 355 nm, then split into two excitation pulses. These excitation pulses are then recombined at the sample, creating the transient grating. The remainder of the pulse-train is frequency doubled to synchronously pump a tunable dye laser whose output probes the grating after a variable delay. The Bragg-diffracted part of the probe pulse is the transient grating signal. PC, Pockels cell; P, polarizer; PD, photodiode; DC, dye cell; E, etalon; BS, beam-splitter.

the I.R. pulse-train to fix the timing between them. The variably delayed dye-laser pulse probes the grating at the Bragg angle. The diffracted intensity, measured with a PIN photodiode and lock-in amplifier, is the signal. In other configurations of the system, the tunable dye pulse is beam-split to form the excitation pulses and one of the Nd:YAG harmonics is used as a probe, or the same colour is used for both excitation and probing.

The same type of mode-locked Nd:YAG and dye-laser equipment is used in the fluorescence mixing experiments. In these experiments, a specific polarization component of the fluorescence decay is directly observed. The setup shown in figure 3 is configured for the experiments on excitation transport among dye molecules in solution (Gochanour and Fayer 1981, Miller *et al.* 1983) (Section 3). A green single pulse at 532 nm excites the sample. The resulting fluorescence is filtered to remove scattered excitation light and focused into an RDP type-I sum-generating crystal where it overlaps with the path of a 1·06-$\mu$m single pulse selected from the YAG laser pulse-train by a Pockels cell and polarizer. The fluorescence reaching the sum crystal coincident in time with the 1·06-$\mu$m pulse mixes with that pulse to produce a short burst of U.V. light ($\sim$365 nm). The U.V. intensity is proportional to the fluorescence intensity at that time. The sum crystal is oriented so that only the component of the fluorescence polarized parallel to the 1·06-$\mu$m polarization is summed. A half-wave plate varies the polarization of the excitation pulse relative to the summing pulse, allowing both the parallel and perpendicular polarization components of the fluorescence ($I_{\parallel}(t)$ and $I_{\perp}(t)$) to be obtained. The excited-state lifetime can be determined directly by adjusting the relative polarization of the excitation and summing pulses to the magic angle (54·7°)



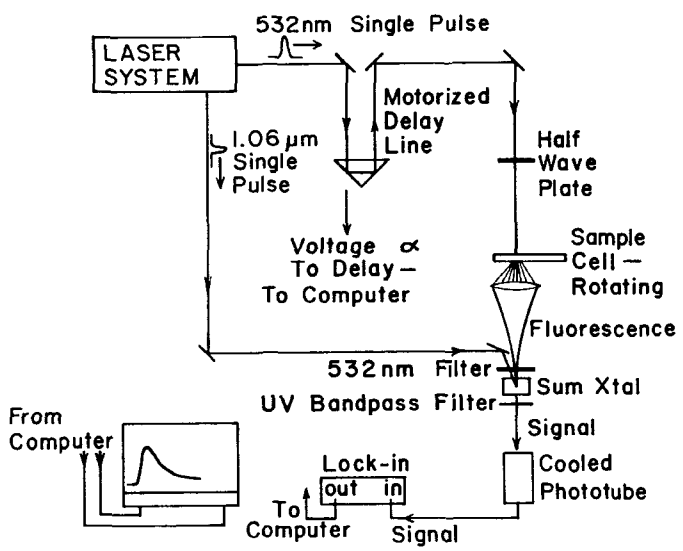


Figure 3. Time-resolved fluorescence mixing experimental setup. The laser system consists of a 500-Hz repetition rate, acousto-optically mode-locked and $Q$-switched Nd:YAG laser. The sample is excited by a 0·532-$\mu$m Nd:YAG second harmonic single pulse. The resulting fluorescence which is time coincident in the summing crystal with a 1·06-$\mu$m Nd:YAG fundamental pulse is summed to produce a U.V. signal pulse which is proportional to the fluorescence at that time. The motorized delay line provides temporal resolution by varying the time between the sample excitation and the fluorescence summing.

(Gochanour and Fayer 1981). At this angle, a signal proportional to the total fluorescence is obtained; that is, depolarization processes do not contribute to the signal.

The time decay is swept out by varying the delay between the excitation pulse and the summing pulse with a motorized delay line. The signal is detected through a U.V. bandpass filter by a cooled photomultiplier. The phototube output is measured with a lock-in amplifier operating at the laser frequency. The lock-in output and a voltage proportional to the delay time are digitized and stored on disc.

## 3. Excitation transport and trapping: chromophores distributed randomly in solution

### 3.1. *Excitation transport*

The transport of electronic excited-state energy among a set of identical molecules randomly distributed in a medium such as a solution or a glass has been a challenging problem for both the theorist and experimentalist. Excited-state transport can lead to such processes as sensitized luminescence and sensitized photochemistry. Förster's (1948) original work employed assumptions that led to the description of excited-state transport as inherently diffusive. This provided a qualitative understanding of the transport phenomenon. A quantitative theory (Gochanour *et al.* 1979) shows that transport is not generally diffusive. The experimental results provide strong support for the theory and give the first complete description of electronic excited-state transport in a random system (Gochanour and Fayer 1981).



An important characteristic of a random system is the statistical distribution of intermolecular distances, which leads to a distribution of transfer rates from an initially excited molecule to surrounding unexcited molecules. There is not a single path by which excitation probability is transferred between two molecules but rather an infinite set of possible paths involving all the molecules in the sample. An ensemble average over this set of paths is necessary to describe the actual transfer process.

Until recently theoretical work on this problem has been limited to the study of very low concentration systems (Craver and Knox 1971, Haan and Zwanzig 1978), the case in which energy transport is close to negligible. In this situation an excited molecule is taken to interact with a small number of neighbouring molecules and is independent of all other molecules in the sample. This approximation is valid when the initial site is the only significant source of excitation probability, that is, the low-concentration, short-time limit. Examples of such calculations include the steady-state fluorescence depolarization calculations of Craver and Knox (1971), the time-dependent fluorescence depolarization calculation of Hemenger and Pearlstein (1973), and the Green function calculation of Haan and Zwanzig (1978).

As mentioned above, a comprehensive theoretical study of excited-state transport in random systems based on a diagrammatic expansion of the Green function has been presented recently (Gochanour *et al.* 1979). In this section, this theoretical treatment will be briefly recounted and the connection to time-resolved fluorescence depolarization experiments (Gochanour and Fayer 1981) will be made. Since the experiments involve molecules with large transition dipoles, the Förster dipole–dipole mechanism will be responsible for excitation transfer. Therefore the theory will be described explicitly for the dipole mechanism, although it can be used with any type of transfer mechanism, e.g., octupole–octupole interactions responsible for excitation transfer in naphthalene mixed crystals (Section 5).

Each configuration of $N$ molecules distributed randomly in a volume $V$ with number density $\rho$ is characterized by the location and orientation of the $N$ molecules $(\mathbf{r}_1, \Omega_1; \mathbf{r}_2, \Omega_2; \ldots; \mathbf{r}_N, \Omega_N)$. The vector $\mathbf{r}_i$ gives the location of molecule $i$ while $\Omega_i$ represents the set of angular coordinates necessary to specify the orientation of the transition dipole. The master equation for each configuration, denoted by $R$, is

$$dp_j(R,t)/dt = -p_j(R,t)/\tau + \sum_k w_{jk}[p_k(R,t) - p_j(R,t)] \tag{1}$$

where $p_j(R,t)$ is the probability that an excitation is found on molecule $j$ in configuration $R$ at time $t$, $\tau$ is the measured lifetime, and $w_{jk}$ is the transfer rate between molecule $j$ and $k$. For the Förster mechanism the $w_{jk}$ are given by

$$w_{jk} = \tfrac{3}{2}\tau^{-1} K_{jk}^2 (R_0/r_{jk})^6 \tag{2}$$

$R_0$ characterizes the strength of the intermolecular interaction and can be determined from steady-state spectroscopy (Förster 1948). Qualitatively, $R_0$ is a measure of the distance over which energy transport is efficient. The orientation factor $K_{jk}^2$ is dependent on the relative orientation of the transition dipoles of molecules $j$ and $k$ and can be written as

$$K_{jk}^2 = [\hat{\mathbf{d}}_j \cdot \hat{\mathbf{d}}_k - 3(\hat{\mathbf{d}}_j \cdot \hat{\mathbf{r}}_{jk})(\hat{\mathbf{d}}_k \cdot \hat{\mathbf{r}}_{jk})]^2 \tag{3}$$

where $\hat{\mathbf{d}}_j$ and $\hat{\mathbf{d}}_k$ are unit vectors in the directions of the transition dipoles of molecules $j$ and $k$ and $\hat{\mathbf{r}}_{jk}$ is a unit vector in the direction of a vector connecting molecule $j$ and $k$.

The quantity most useful for obtaining information concerning transport is the Green function:

$$G(\mathbf{r} - \mathbf{r}', t) = G^{\mathrm{s}}(t) + G^{\mathrm{m}}(\mathbf{r} - \mathbf{r}', t) \tag{4}$$

The Green function can be thought of as the probability of finding an excitation at position $\mathbf{r}$ and time $t$ with the initial condition of unit probability at $\mathbf{r}'$. It is convenient to divide the Green function into two terms, one which is a measure of probability at the initial site of excitation $\mathbf{r}'$, $G^{\mathrm{s}}(t)$, and one which is a measure of the probability found on a molecule a distance $\mathbf{r} - \mathbf{r}'$ from the initial site, $G^{\mathrm{m}}(\mathbf{r} - \mathbf{r}', t)$.

The two components of the Green function can be expanded in diagrammatic series. To do this it is convenient to work with the Fourier–Laplace transforms of $G^{\mathrm{s}}(t)$ and $G^{\mathrm{m}}(r - r', t)$, $\hat{G}^{\mathrm{s}}(\varepsilon)$ and $\hat{G}^{\mathrm{m}}(\mathbf{k}, \varepsilon)$. The diagrammatic series corresponding to each of these functions is obtained by expanding the functions in powers of $\varepsilon$ and $w_{jk}$. An infinite series of products of $w_{jk}$ factors results. Each of these products is then associated with a diagram. The complexity of the diagrammatic series can be decreased through a topological reduction. This procedure involves examination of the topological structure of the $\hat{G}(\mathbf{k}, \varepsilon)$ diagrammatic series to find a smaller set of $\hat{G}^{\mathrm{m}}(\mathbf{k}, \varepsilon)$ diagrams from which all diagrams can be generated. The resulting series of diagrams, the $\tilde{\Sigma}(\mathbf{k}, G^{\mathrm{s}}(\varepsilon))$ series, is both a function of $\hat{G}^{\mathrm{s}}(\varepsilon)$ and can be used to generate $\hat{G}^{\mathrm{s}}(\varepsilon)$. Conservation of probability implies a self-consistent condition which is used to generate an approximate solution for the Green function.

The results of the diagrammatic method reproduce analytically the low-concentration, short-time theoretical results of Haan and Zwanzig (1978). In addition, the calculations yield information on the system's intermediate and long-time behaviour. The results show that, for all concentrations, excited-state transport becomes diffusive at sufficiently long times. The long-time diffusion constant is given by

$$D = 0{\cdot}374 C^{4/3} R_0^2 \tau^{-1} \tag{5}$$

This value is in good agreement with the result from Förster's (1948) simple model of equally spaced chromophores. However, the recent results show that for low-concentration systems, transport becomes diffusive only at very long times, i.e., after more than a few lifetimes, and thus for all practical purposes transport is not diffusive. For high concentrations transport becomes diffusive within one lifetime.

If a solution of molecules in a viscous solvent is irradiated with a short pulse of polarized light, molecules with their transition dipoles oriented parallel to the excitation polarization are preferentially excited. If the ensuing fluorescence is detected through a polarizer, the initial ratio of parallel polarized fluorescence intensity to perpendicular polarized intensity is 3 : 1. In a low-concentration sample where energy transfer does not occur, both components of the fluorescence decay with the lifetime and the polarization ratio is preserved. In higher-concentration samples excited-state population is transferred to randomly oriented molecules and the fluorescence is depolarized. Galanin has shown that the overwhelming contribution to fluorescence polarization is due to fluorescence from chromophores which were initially excited (Craver and Knox 1971, Galanin 1950, Jabloński 1970), that is, energy transfer can be assumed to occur to a randomly oriented molecule. Thus the time dependence of fluorescence depolarization will be related to the time-dependent probability that the excitation is at the initial site. For the theoretical model described here, this probability is given by the inverse Laplace transform of $\hat{G}^s(\varepsilon)$, which will be denoted by $G^s(t)$. $\hat{G}^s(\varepsilon)$ is given by

$$\hat{G}^s(\varepsilon)=\tau\{(\pi^2\gamma^2C^2/4)[1-[1+(32/\pi^2\gamma^2C^2)(\varepsilon\tau-0{\cdot}1887\gamma^2C^2)]^{1/2}] + 4(\varepsilon\tau-0{\cdot}1887\gamma^2C^2)\}/[4(\varepsilon\tau-0{\cdot}1887\gamma^2C^2)^2] \quad (6)$$

where the dimensionless concentration $C$ is given by

$$C=\tfrac{4}{3}\pi R_0^3\rho \quad (7)$$

$$\gamma=0{\cdot}846 \quad (8)$$

and $\rho$ is the number density. $G^s(t)$ is obtained from equation (6) by numerical inversion of the Laplace transform (Stehfest 1970).

Thus the fluorescence arises from two ensembles. The first, with a weighting factor $G^s(t)$, consists of molecules initially excited and the resulting fluorescence is polarized. The second ensemble, with a weighting factor $\{1-G^s(t)\}$, consists of molecules to which excited-state energy has been transferred; the fluorescence from these sites is unpolarized. Calculation of the component of the fluorescence with a given polarization for each of these ensembles is straightforward. The following results are obtained

$$I_{\parallel}(t)=\exp(-t/\tau)\{1+0{\cdot}8G^s(t)\} \quad (9\,a)$$

$$I_{\perp}(t)=\exp(-t/\tau)\{1-0{\cdot}4G^s(t)\} \quad (9\,b)$$

where $I_{\parallel}$ and $I_{\perp}$ are the fluorescence intensities polarized parallel and perpendicular to the excitation polarization. Equations (9 *a*) and (9 *b*) show the direct path from the experimental observables to the system's Green function and thus to a detailed description of the excited-state transport.

Solutions of rhodamine 6G (R6G) in glycerol were studied using the fluorescence mixing method described in Section 2 to measure the time-resolved fluorescence depolarization (Gochanour and Fayer 1981). The fluorescence mixing technique permits examination of $I_{\parallel}$ and $I_{\perp}$.

Sample excitation was by 532-nm, 50-ps pulses. The samples consisted of known concentrations of R6G dissolved in glycerol. The solution is placed in a rotating sample cell of approximately 5·0 cm diameter formed by two glass flats separated by thin foil spacers. The sample cell is rotated to avoid effects due to photodecomposition or heating. The cell thickness was adjusted from 300 to 5 $\mu$m to control the optical density of the various concentration samples in order to eliminate reabsorption problems.

First a low-concentration sample ($2{\cdot}95 \times 10^{-5}$ M) was examined. This sample corresponds to the $C = 0{\cdot}0$ limit, that is, excited-state transport is negligible. The decays of the parallel and perpendicular components of the fluorescence are identical; they decay exponentially with a lifetime of $3{\cdot}1 \pm 0{\cdot}1$ ns. In addition to providing the lifetime which is a necessary input for the theory, the low-concentration data demonstrate that molecular rotation is much slower than the lifetime and thus depolarization effects due to molecular rotation (Chuang and Eisenthal 1971, Porter *et al.* 1977, Moog *et al.* 1982) do not occur on the time scale of the experiment.

The effect of increasing concentration can be seen in the data in figure 4. For a concentration of $2{\cdot}6 \times 10^{-3}$ M the decay of the parallel component of the fluorescence is found to be faster than the 3·1-ns exponential decay obtained at low concentration while the decay of the perpendicular component is slower than the lifetime decay. The



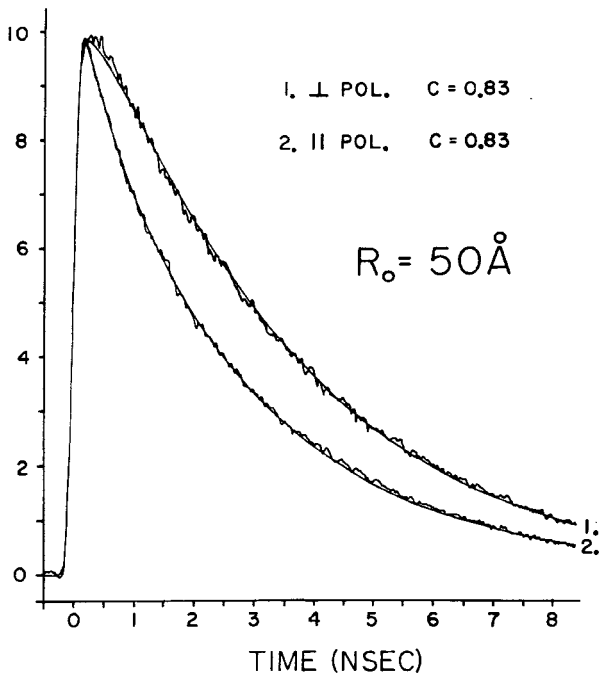


Figure 4. Depolarization data and theoretical curves for a sample of rhodamine 6G (R6G) in glycerol of concentration $2{\cdot}6 \times 10^{-3}$ M. The decay of the parallel component is faster than the lifetime decay and the decay of the perpendicular component slower than the lifetime decay due to excited-state transport-induced depolarization. The Förster radius, $R_0 = 50$ Å, was determined spectroscopically. The solid curves through the data were calculated theoretically using equations 9(*a*) and (*b*) *without recourse to adjustable parameters.*

value of the Förster radius, $R_0$, was determined from the overlap of the absorption and fluorescence spectra (Förster 1948). For R6G in glycerol, $R_0 = 50$ Å. Since the sample lifetime, $\tau$, the sample concentration, and $R_0$ are all known, all the parameters necessary for the theoretical calculation of the time-dependent depolarization due to excitation transport are available. The solid curves through the data were calculated using equations (9 *a*) and (9 *b*) *without recourse to adjustable parameters.*

In figure 5, the decay of the parallel component of the fluorescence is shown for solutions having reduced concentrations of $C = 0{\cdot}5$ and $C = 1{\cdot}7$. The solid lines through the data points are the theoretical curves calculated for these concentrations. The agreement between the experimental data and the theoretical curves (no adjustable parameters) is nearly perfect for both concentrations. Similar agreement has been obtained for the decay of the perpendicular component of the fluorescence decay. The same quality of agreement was also obtained for a range of sample concentrations. These results confirm the accuracy of the diagrammatic self-consistent theoretical method and yield a comprehensive description of excited-state transport in solution.

Using the experimental results with the diagrammatic theory it is possible to calculate any of the energy transport properties of the system studied. One of the most important results of the theory is that excitation transport among chromophores randomly distributed in solution is nondiffusive at short time and becomes diffusive in



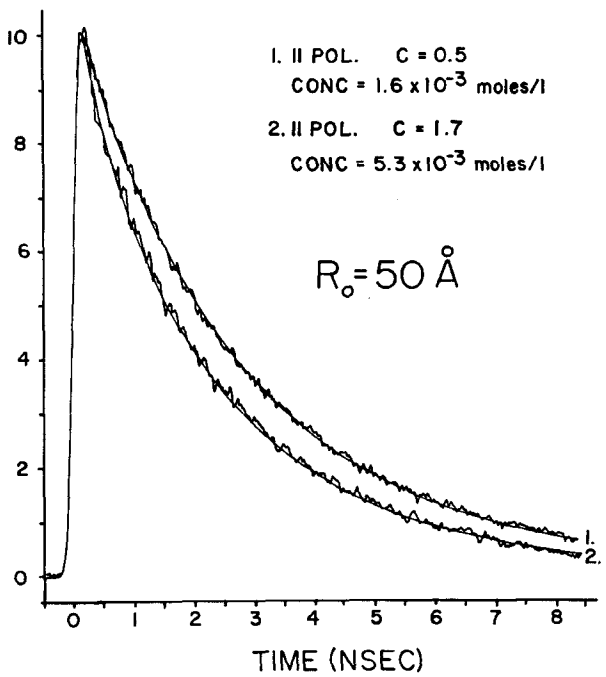


Figure 5. Depolarization data and theoretical curves for the parallel component of the fluorescence of rhodamine 6G (R6G) in glycerol for concentrations corresponding to $C = 0{\cdot}5$ and $C = 1{\cdot}7$. The theoretical curves for these concentrations were calculated with no adjustable parameters. The agreement between theory and experiment is near perfect. The same quality of agreement was obtained for a variety of sample concentrations. These results confirm the diagrammatic self-consistent theoretical method and yield a comprehensive description of excited-state transport.

the long-time limit. If transport is diffusive, the mean-square displacement of the excitation increases linearly in time. The time derivative of the mean-square displacement is then a constant, $6D$, where $D$ is the diffusion constant (see equation (5)). In figure 6 the time derivatives of the mean-squared displacements are displayed for reduced concentrations (equation (7)) $C=0{\cdot}5$, $C=1{\cdot}7$ and $C=5{\cdot}0$. (To illustrate the transport properties of the system, the curves are calculated without the exponential decay due to the lifetime.) For $C=0{\cdot}5$, a relatively low concentration, transport is nondiffusive for the 2·5 lifetimes displayed in the graph. For $C=1{\cdot}7$, a moderate concentration, transport is approaching the diffusive limit by 2·5 lifetimes. For $C=5{\cdot}0$, a moderately high concentration, transport, although highly nondiffusive at short time, becomes diffusive by $\sim 3/4$ lifetimes.

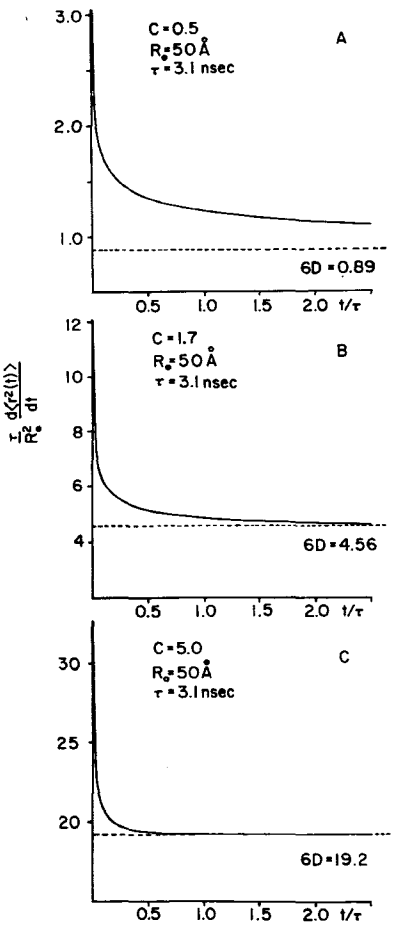


Figure 6. Calculated time derivatives of the mean-square displacement of an excitation undergoing transfer between molecules randomly distributed in solution. The parameters $R_0$ and $\tau$ are appropriate for the system studied, R6G in glycerol. The dashed lines indicate the theoretical value of the long-time-limit diffusion rate. For $C=0{\cdot}5$ (figure 6(*a*)) transport is not diffusive during the first several lifetimes. For $C=1{\cdot}7$ (figure 6(*b*)) transport is approaching the diffusive limit by two lifetimes. For $C=5{\cdot}0$ (figure 6(*c*)) transport becomes diffusive within one excited-state lifetime.

Calculation of mean-square displacements yields interesting information concerning the transport of the excitation. For $C=1{\cdot}7$ and $t=\tau$, the root mean-square displacement is 117 Å. This corresponds to a volume in which the average number of molecules is about 21. For $t=2\tau$ the excitation is distributed over a volume in which the average number of molecules is 50. Even for this relatively low concentration, it is clear that theoretical treatments which allow transfer among only two or three near neighbours are inadequate to describe the transport properties of a random system over full ranges of time and concentration.

### 3.2. *Transport and trapping*.

The experiments and theory described above apply to systems with a single type of chromophore. Hence, there is only donor–donor excitation transport. Another important class of energy transport problems involves systems with two types of chromophores, donors and traps. Excitation transport occurs among the donors and transfer from donors to traps can also occur. However, transfer to the traps is irreversible, usually because the trap is lower in energy and energy dissipation upon trapping makes back transfer to a donor energetically impossible. For example, this is the situation in a photosynthetic unit in which energy transport among chlorophyll molecules leads to irreversible trapping of the energy on the reaction centre (Beddard and Porter 1976, Sauer 1978).

Förster treated the trapping problem in an important limiting case, which we refer to as the Förster limit (Förster 1949). The Förster limit involves a two-component ensemble of donor and trap molecules in the regime of high trap concentration and near-zero donor concentration. Since each donor is surrounded by many traps, the excitation probability flows directly from a donor to the traps with no donor–donor transport. This greatly simplified the problem and allowed an exact theoretical solution. The basic applicability of this result to an experimental system investigated on a picosecond time scale was first demonstrated by Rehm and Eisenthal (1971). Although the Förster theory is useful within its restrictions, it is not extendable to other concentration regimes. Many types of systems of experimental interest occur outside the low-donor-concentration limit. Transport among chromophores in polymer coils and eventual trapping by excimers (Klöpffer 1981, Frank and Harrah 1974) (e.g. polyvinylnaphthalene), transport and trapping in photosynthetic units (Pearlstein 1964, Markvart 1978, Porter 1978), ruby crystals (Selzer *et al.* 1977, Imbusch 1967), or concentrated dye solutions (Lutz *et al.* 1981), and similar problems involving electron transport (Scher *et al.* 1980), are but a few examples of important current problems requiring a broader understanding of transport phenomena in disordered systems.

Loring, Andersen and Fayer (LAF) (1982a, b) extended the diagrammatic approach of Gochanour, Andersen and Fayer (GAF) (1979) described in the previous section. LAF treated two-component systems composed of donors and traps. Again an accurate approximation for the Green function solution to the system's master equation is obtained. The LAF results permit calculation of experimental observables at all times and for any combination of donor and trap concentration. It accurately reproduces the Förster limit results for very low donor concentration and high trap concentration. It recovers the results of GAF in the opposite limit, that is, high donor concentration and zero trap concentration. For intermediate cases the LAF treatment provides an accurate description of transport and trapping in disordered systems.

In the experiments described below, the time-dependent excited-donor population is monitored. Thus we need an expression for $G^{D}(t)$, the part of the Green function that

gives the time-dependent probability of finding an excitation in the donor ensemble, given that an excitation is created in the donor ensemble at $t=0$. The decay of $G^{D}(t)$ will be determined by the transport dynamics which depend on the donor and trap concentrations and the strengths of the donor–donor and donor–trap interactions ($R_0^{DD}$ and $R_0^{DT}$). The theoretical development of LAF gives an expression for $G^{D}(\varepsilon)$, the Laplace transform of $G^{D}(t)$. This expression is a function of $C_D$ and $C_T$ where

$$C_D = \tfrac{4}{3}\pi R_0^{DD^3}\rho_D \tag{10a}$$

and

$$C_T = \tfrac{4}{3}\pi R_0^{DT^3}\rho_T \tag{10b}$$

$C_D$ and $C_T$ are the reduced concentrations and $\rho_D$ and $\rho_T$ are the number densities for donors and traps, respectively. $R_0^{DD}$ (donor–donor) and $R_0^{DT}$ (donor–trap) are lengths which characterize the excited-state intermolecular transfer interactions (Förster 1948). (In the last section only donor–donor transport was considered. Therefore it was unnecessary to use subscripts and superscripts to distinguish donor and trap parameters.) As in the experiments described above, $R_0^{DD}$ and $R_0^{DT}$ can be determined spectroscopically.

The LAF formalism provides an analytical expression for $\hat{G}^{D}(\varepsilon)$, the Laplace transform of the probability of finding the excitation in the donor ensemble, i.e., of finding an excitation which has not trapped. This expression does not include loss of donor probability due to decay of the donor to its ground state. To obtain an expression for use in comparison with experiments (Loring *et al.* 1982 a, b), first $\hat{G}^{D}(\varepsilon)$ is numerically inverted to give $G^{D}(t)$. $G^{D}(t)$ is then multiplied by a decaying exponential to account for the donor excited-state lifetime, i.e.,

$$N^{D}(t) = G^{D}(t)\exp(-t/\tau_D) \tag{11}$$

where $N^{D}(t)$ is the number of excited donor molecules as a function of time. $N^{D}(t)$ is directly proportional to the time-resolved fluorescence decay, the experimental observable in the fluorescence mixing experiments. It is also the observable in transient grating and probe-pulse experiments. All three techniques were employed to examine the transport and trapping problem experimentally (Miller *et al.* 1983). Only data from fluorescence mixing experiments will be discussed here.

In the experiments described below, the donor is R6G and the trap is malachite green (MG). MG in room temperature solutions has a negligible quantum yield and a picosecond time scale lifetime. Therefore, an excitation which leaves the donor ensemble by trapping does not contribute to the fluorescence. The sample is excited with 532-nm light. The excitation pulse was polarized at $54{\cdot}7 \pm 0{\cdot}5^{\circ}$ (the magic angle) with respect to the I.R. single pulse and the sum crystal axis to eliminate fluorescence depolarization effects arising from molecular rotation (Chuang and Eisenthal 1971, Porter *et al.* 1977, Moog *et al.* 1982) or excited state transport (Gochanour and Fayer 1981). Again samples were studied in a rotating cell to avoid heat and photodecomposition problems. Studies of sample thickness were made to ensure that reabsorption did not influence the experimental results. It was found that an optical density of 0·06 or less, at 0·532 $\mu$m, the absorption peak, would eliminate reabsorption problems in the system studied. The intensity of laser excitation was attenuated by a series of neutral density filters until stimulated emission and other power-dependent effects were eliminated.

In figure 7, experimental data from various R6G-MG systems are displayed. The donor lifetime, $\tau_D$, was measured in a low concentration sample. Given $\tau_D$, the only remaining parameters in the LAF theory are $R_0^{DT}$ abd $R_0^{DD}$. These were determined independently from the overlap of the fluorescence spectra of R6G with the absorption spectra of R6G and MG. As a first test of procedures and to confirm the spectroscopic measurements, the Förster limit was studied and $R_0^{DT}$ was obtained. The results of the fluorescence mixing studies are shown in figure 7(*a*). The MG concentrations were

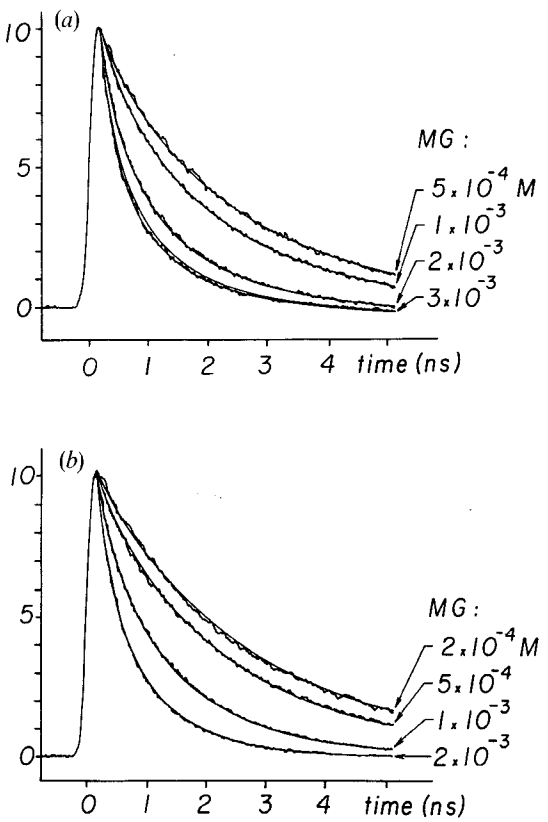


Figure 7. Time-resolved fluorescence mixing data for rhodamine 6G (R6G) and malachite green (MG) in ethanol. (*a*) The Förster limit. The R6G concentration is low ($1 \times 10^{-4}$ M) and the MG concentrations (indicated) are high. Only donor to trap energy transport occurs. The solid curves through the data were calculated using $R_0^{DT}$ as an adjustable parameter. For all curves, $R_0^{DT}$ is $58 \pm 1$ Å. The sensitivity of the calculation to $R_0^{DT}$ is illustrated by the two solid lines for the $3 \times 10^{-3}$ M data. The upper solid line was calculated with $R_0^{DT} = 57$ Å while the curve through the data has $R_0^{DT} = 58$ Å. The time-resolved measurement of $R_0^{DT}$ agrees well with the spectral overlap measurement of $59 \pm 1$ Å. (*b*) Higher donor concentration systems. At this R6G concentration ($3 \times 10^{-3}$) the effects of donor–donor energy transport become appreciable. The solid curves through the data were calculated with the LAF theory without adjustable parameters using the independently determined values of $R_0^{DT}$, $R_0^{DD}$, and $\tau_D$. Excellent agreement between theory and experiment is obtained for other concentrations of R6G and MG as well.

varied from $5 \times 10^{-4}$ M to $3 \times 10^{-3}$ M with R6G concentrations of $1 \times 10^{-4}$ M. Higher concentrations of MG than $3 \times 10^{-3}$ M absorbed almost all the fluorescence, making the signal-to-noise ratio too low to be useful. The solid lines through the data were obtained from equation (11). The reduced donor concentration was $C_D = 0{\cdot}02$ (no donor–donor transport). $R_0^{DT}$ was used as an adjustable parameter to obtain the calculated curves in figure 7(*a*). All the concentrations were fit with a single value of $R_0^{DT} = 58 \pm 1$ Å. The accuracy of this measurement is demonstrated in figure 7(*a*) for the MG concentration of $3 \times 10^{-3}$ M. The top solid curve is calculated with an $R_0^{DT}$ of 57 Å while the curve running through the data has an $R_0^{DT}$ of 58 Å. The calculated curve with $R_0^{DT} = 59$ Å (not shown) is symmetrically displaced from the 58 Å curve. The measurement of $R_0^{DT}(= 58$ Å) is in excellent agreement with the spectral measurement which found $R_0^{DT} = 59 \pm 1$ Å. The close agreement between the spectroscopically determined value of $R_0^{DT}$ and the time-resolved measurements over a wide range of concentrations supports the accuracies of the determinations. To check for systematic errors in our time-resolved measurements, we repeated the Förster limit concentration studies using transient grating and probe pulse techniques at two different excitation wavelengths, 0·532 and 0·355 $\mu$m. The results were very close to those obtained from the fluorescence mixing experiments, with the probe pulse and transient grating measuring $R_0^{DT} = 57 \pm 1$ Å and $R_0^{DT} = 58 \pm 2$ Å, respectively.

Figure 7(*b*) displays fluorescence mixing data for a series of experiments on the general transport and trapping problem in which the donor concentration and donor–donor transport are significant. The curves are for fixed R6G donor concentration. The solid lines through the data are calculated using equation (11) with no adjustable parameters. The agreement between experiment and theory is very good. Equally good agreement was obtained for systems in which the R6G concentrations was $2 \times 10^{-3}$ M and $1 \times 10^{-3}$ M. The effect of donor–donor transport is significant as can be seen by comparing the results in figure 7(*b*) to the Förster limit results having the same MG concentrations. For example, $\tau_{eff}$ (the time required for the signal to fall to $1/e$) for $1 \times 10^{-3}$ MG samples in the Förster limit is $\sim 2$ ns (figure 7(*a*)). The same MG concentration, but with a RG6 concentration of $3 \times 10^{-3}$ M, has a $\tau_{eff}$ of $\sim 1{\cdot}4$ ns (figure 7(*b*)). At higher concentrations of R6G, transient grating experiments were used to avoid reabsorption problems. Experiments were also performed in glycerol to examine the theory's capacity for handling fixed molecular orientations as well as rapidly rotating molecules. These two situations require different angular ensemble averages of the Green function (Gochanour and Fayer 1981). In all cases the diagrammatic theory is able to reproduce the experimental results without recourse to adjustable parameters.

Theoretical problems associated with excited-state transport phenomena have both quantum mechanical and statistical mechanical aspects. Förster (1948, 1949) and subsequent workers (Dexter 1953, Vavilov and Galanin 1949) have accurately related spectroscopic observables to the intermolecular interactions and transfer rate between a pair of molecules. However, it is the interplay of intermolecular interactions among a large number of molecules that determines the nature of excited-state transport in solution. In any microscopic volume, there is a fixed spatial arrangement of atoms or molecules which controls the local time evolution of energy transport. A macroscopic solution contains an infinite collection of all possible local environments. Thus, the time-resolved observables of energy transport in solution involve an infinite number of dynamic systems. Owing to the recent theoretical and experimental advances, we now have a detailed understanding of excitation transport in such disordered media.

## 4. Fluorescence quenching in concentrated dye solutions

A common situation in which excitation transport and trapping occurs in solution is in the process of fluorescence quenching in concentrated dye solutions. This is a well known phenomenon in which the apparent fluorescence quantum yields of dye solutions drop dramatically at very high dye concentration. Recent work reveals the underlying dynamic mechanism responsible for fluorescence quenching.

The experimental evidence suggests that three radiationless processes govern the disposition of electronic excited-state energy in concentrated dye solutions. These three processes are energy transfer between dye molecules (Gochanour *et al.* 1979, Hetherington *et al.* 1979), trapping by dimers (Loring *et al.* 1982 a, b, Imbush 1967), which have states of lower energy, and radiationless relaxation (Birks 1970) of the dimer excited state. A simple model provides a microscopic dynamical picture of fluorescence quenching (Schäfer 1977) in concentrated dye solutions. Qualitatively, the concentration-dependent processes that combine and result in fluorescence quenching work in the following manner. At very low concentration, a dye solution absorbs light and fluoresces. At moderate concentrations, electronic excited-state energy transport occurs due to dipole–dipole interactions between the dye molecules (Berlmann 1973).The energy transport causes fluorescence depolarization effects, as discussed above (Gochanour and Fayer 1981), but does not affect —the fluorescence quantum yield. As the concentration is increased further, ground state dimer formation begins (Selwyn and Steinfeld 1972, Bojarski *et al.* 1975) and the rate of energy transport continues to increase. By dimers we mean aggregates of two dye molecules that have distinct spectral and other characteristics. Rapid transport among the monomers allows an excitation to find a dimer and become trapped on it. The experiments indicate that back transfer from the excited dimer to monomers is negligible. Once the excitation is trapped on a dimer, rapid radiationless relaxation to the ground state occurs and the fluorescence is quenched.



The concentration dependence of the fluorescence quenching is determined by the concentration dependence of the trapping. The trapping rate depends on both the dimer concentration and the concentration-dependent rate of energy transport. The model predicts that the trapping rate varies approximately as the cube of the dye concentration. Therefore the onset of fluorescence quenching with increasing concentration is very rapid.

Experimentally, the onset of trapping by dimers manifests itself as an apparent reduction in the excited-state lifetime. In the limit, that energy transport becomes extremely rapid, the trapping occurs on a time scale that is short relative to the dimer lifetime, and the excited-state population decays with the dimer lifetime. In the two systems studied, rhodamine 6G (R6G) in glycerol and R6G in ethanol, the dimer lifetimes are 830 ps and $<50$ ps, respectively. Presumably, the dimers have faster radiationless relaxation rates than the monomers because of the loose nature of the dimer complexes. The dimers undergo rapid configurational changes that enhance the radiationless relaxation rates. This is consistent with the longer dimer lifetime in the glycerol solvent. Since glycerol is much more viscous than ethanol, it will 'hold' the dimer complex more rigidly and therefore will slow radiationless relaxation.

A formally correct, accurate treatment of this problem involves the solution of the master equation for excited-state transport and trapping in an ensemble of randomly distributed dye molecules and dimer traps in solution (Loring *et al.* 1982 a, b). This approach was discussed in the last section. As the mathematical complexity of the accurate treatment would obscure the basic nature of the problem, we will employ an

heuristic, qualitatively correct, analysis (Lutz *et al.* 1981) in terms of a simple set of rate equations. These rate equations employ a trapping rate constant. The full diagrammatic Green function treatment confirms the basic concentration dependence presented here; however, trapping is not governed by a rate constant but involves a time-dependent trapping rate function. Thus the detailed time development of these equations is not correct.

In the simple model, the rate equations governing the excited state populations are:

$$dM^*/dt = -K_M M^* - K_T M^* \tag{12a}$$

$$dD^*/dt = -K_D D^* + K_T M^* \tag{12b}$$

$M^*$ is the concentration of excited monomers and $D^*$ is the concentration of excited dimers. $K_M$ is the rate constant for decay of excited monomers to the ground state by radiative and nonradiative processes and $K_D$ is the analogous rate constant for decay of dimers to the dimer ground state. $K_T$ is the trapping rate constant.

The experiments were performed with the transient grating method to minimize reabsorption problems in the high-concentration samples. The transient grating signal depends on the square of the excited state concentration (Fayer 1982) $\{N_1(t)\}^2$, i.e.

$$S(t) = A\{N_1(t)\}^2 \tag{13}$$

where $A$ contains all the time-independent parameters such as beam geometries and $N_1(t) = M^* + D^*$, the sum of the excited monomer and dimer concentrations. Solution of the rate equations yields

$$N_1(t) = M_0^*(\exp[-(K_M + K_T)t] + [K_T/(K_M + K_T - K_D)] \times \{\exp(-K_D t) - \exp[-(K_M + K_T)t]\}) \tag{14}$$

$N_1(t)$ is the time-dependent function determined experimentally from $S(t)$. It is informative to note some special cases of equation (14). If $K_T$ is very small, trapping is negligible and $N_1(t)$ decays exponentially with the monomer rate constant, $K_M$. If $K_D \gg K_M, K_T$, then $N_1(t)$ decays exponentially with a rate constant $(K_M + K_T)$. And if $K_T \gg K_M, K_D$, excitations are immediately trapped by dimers and $N_1(t)$ decays exponentially with the dimer rate constant, $K_D$.

In general, trapping is characterized by a time-dependent trapping rate function (Loring *et al.* 1982 a, b, Wieting *et al.* 1978), not by a rate constant. Trapping occurs when an excitation has visited enough distinct sites so that on the average it has sampled one trap species. For a random walk on an isotropic three-dimensional lattice, the number of distinct sites visited increases linearly with time (Montroll 1964). Therefore, trapping can be characterized by a trapping rate constant which depends on the site-to-site hopping time. To improve this approximation, the randomness in spatial distribution of the dye molecules in solution is taken into consideration in the calculation of the hopping time. In using a trapping rate constant we are here treating a solution with its inherent disorder as a lattice. At high concentrations where trapping by dimers is important, transport becomes diffusive very quickly (see figure 6) and is isotropic in the three dimensions. The above considerations lead to the following expression for the trapping rate constant, (Lutz *et al.* 1981), $K_T$:

$$K_T = \left(\frac{Pq}{h_1 M_1^2}\right) M^3 \tag{15}$$

$K_T$ depends on the cube of the dye concentration, $M$. The other parameters are

constants: $q$ is the monomer–dimer equilibrium constant; $h_1$ is the site-to-site hopping time and $M_1$ is the dye concentration, both for a solution with the Förster dimensionless concentration, $C=1$ (see equation 7); $P$ is the probability that on any step a distinct site is visited and corrects for the return to previously visited sites. For an isotropic three-dimensional random walk on a lattice, $P=0{\cdot}66$. The cubic dependence on concentration of the trapping rate constant leads to a very rapid increase in trapping with concentration.

Examination of $N_1(t)$, equation (14), which gives the time-dependent signal, shows that in general the decays are nonexponential. In the data analysis the following procedure is employed. The experimental decays are plotted and a decay constant is determined for each concentration. These are then compared with a theoretical effective decay constant, $K_{\text{eff}}$, obtained from equation (14) by finding the time required for $N_1(t)$ to fall to $1/e$. Thus

$$K_{\text{eff}}=1/t^{\dagger} \tag{16}$$

with $t^{\dagger}$ obtained from equation (14) by

$$N_1(t^{\dagger})=(1/e)\{N_1(0)\} \tag{17}$$

Transient grating experiments were performed on a series of solutions of rhodamine 6G in glycerol ranging in concentration from $8{\cdot}7\times10^{-4}$ M to 0·05 M. A typical result and log plot are shown in figure 8. In all cases the data appeared to decay exponentially for several lifetimes. Thus, the decay could be characterized by an effective rate constant, $K_{\text{eff}}$, as discussed above. A plot of $K_{\text{eff}}$ versus R6G concentration is shown in figure 9. First consider the qualitative features of the concentration dependence. At low concentration, $K_{\text{eff}}$ is independent of concentration and is given by the monomer decay rate: $K_{\text{eff}}=K_{\text{M}}=3{\cdot}3\times10^{8}\,\text{s}^{-1}$. This represents the limit $K_{\text{T}}=0$, no trapping, since there



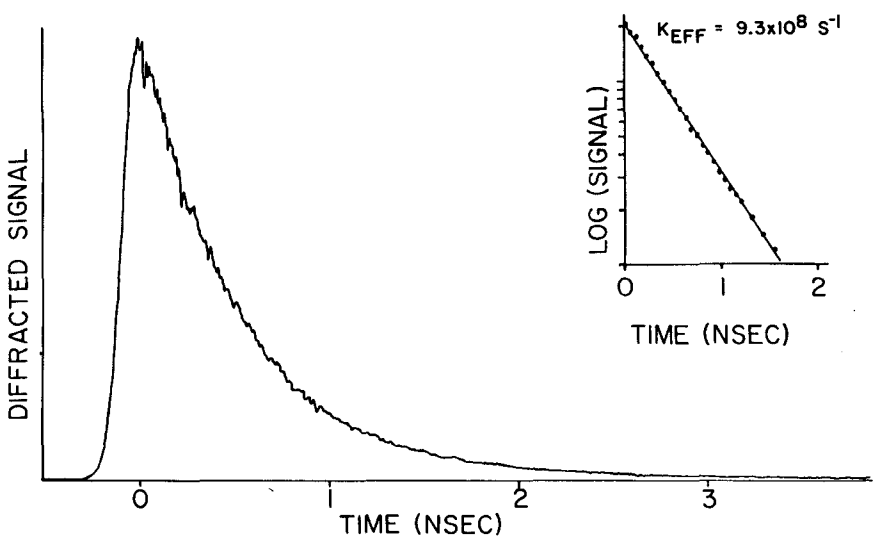


Figure 8. Transient grating results for concentrated rhodamine 6G in glycerol ($1{\cdot}74\times10^{-2}$ M). Probe wavelength, 560 nm. Inset shows the log of the data versus time. The effective decay constant for this data set is $K_{\text{eff}}=9{\cdot}3\times10^{8}\,\text{s}^{-1}$.

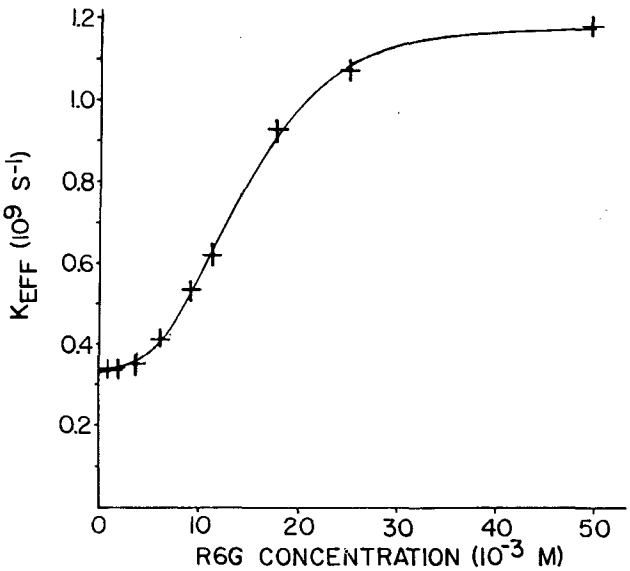


Figure 9. Effective decay constants, $K_{eff}$ versus concentration of rhodamine 6G in glycerol. + indicates experimental data. As the R6G concentration increases, excited-state transport and trapping by R6G dimers becomes increasingly rapid. Fast radiationless relaxation by the dimers decreases the excited-state lifetime and quenches fluorescence. The solid curve is calculated.



are few dimers and transport is relatively slow. At high concentration, $K_{eff}$ is essentially concentration independent and given by the dimer decay rate: $K_{eff} \approx K_D = 1{\cdot}2 \times 10^9\ s^{-1}$ and the dimer lifetime is 830 ps. This corresponds to the limiting case $K_T \gg K_D, K_M$ (instantaneous trapping), which occurs at high concentration since the dimer population is substantial and energy transfer is fast.

In addition to affecting excited-state dynamical processes, dimer formation should give rise to changes in the ground-state absorption spectra of the solutions (Selwyn and Steinfeld 1972, Bojarski *et al.* 1975). Spectra of solutions of many concentrations were examined and it was found that the onset of spectral changes coincides with the onset of changes in the excited-state decay rate. This clearly demonstrates that the concentration dependence of the decay rate is due to changes in the ground-state molecules and not to processes such as excimer formation that only affect the excited states.

Detailed comparison of the model and the experimental data is given in figure 9. The monomer and dimer decay rates were determined from the transient grating (TG) data at low and high concentration, respectively. Since the exact equilibrium constant, $q$, is not known, TG data at a single intermediate concentration was used to determine $K_T$. Decay constants, $K_{eff}$, were then calculated at other concentrations by scaling $K_T$ as the concentration cubed and using equation (14). The calculated values of $K_{eff}$ as a function of concentration yielded the curve (solid line) shown in figure 9. The curve fits the experimentally measured decay constants over the range of concentration, indicating that the microscopic model is basically correct.

Knowing $K_T$ allows calculation of the equilibrium constant for dimer formation from equation (14) since the other parameters are known. An equilibrium constant $q = 9{\cdot}7\,M^{-1}$ was obtained. Equilibrium constants for various solutions of R6G in glycerol–water mixtures have been determined from concentration-dependent absorption spectra to range from $28\,M^{-1}$ in the solution with the most water to $11\,M^{-1}$ in the solution with the least water (Bojarski *et al.* 1975). The equilibrium constant that resulted from the time-dependent measurements is consistent with these values. This provides additional support for the basic model.

Similar experiments were performed for the system R6G in ethanol (Lutz *et al.* 1981). At low concentration the rate constant is determined by the monomer decay rate: $K_{eff} = K_M = 2{\cdot}7 \times 10^8\,s^{-1}$. As the concentration rises, the decay rate rapidly increases. The measurement at the highest concentration is instrumentally limited by the laser pulse duration. The excited-state decay constant at high concentration is at least $2 \times 10^{10}\,s^{-1}$, i.e. the lifetime is less than 50 ps. This is in marked contrast to the glycerol solutions in which the dimer lifetime is 830 ps.

Clearly the radiationless relaxation rates of the loosely bound dimer are influenced by the solvent viscosity. The low viscosity of ethanol permits rapid configurational fluctuations that lead to very fast radiationless relaxation. The fluctuations occur more slowly in glycerol, and thus the dimer lifetime is longer.

These results directly apply to concentration-dependent fluorescence quenching in dye solutions. Trapping on dimers, which increases as the cube of the dye concentration, leads to fast radiationless relaxation and this quenches fluorescence. The solvent-dependent dimer lifetime also influences fluorescence quenching. In high-concentration R6G in ethanol solutions, fluorescence is completely quenched since the dimer radiationless relaxation rate is extremely fast. In high-concentration glycerol solutions, fluorescence is only partially quenched since the dimer decay rate is only four times faster than the monomer decay rate. This allows some radiative relaxation to occur.



## 5. Energy transport on a lattice

### 5.1. *Theory*

All the physical systems involving energy transport which we have discussed in this paper have a common feature. In each case, **r**, the variable that specifies a chromophore's position, has been a continuous variable. We now wish to consider a class of problems where **r** is a discrete variable, and hence the interacting molecules are confined to the sites of a lattice. A theory which considers the discrete structure of a lattice is necessary for a detailed understanding of energy transport in a variety of systems such as mixed molecular crystals. (Gentry and Kopelman 1983, Kopelman 1981, Smith *et al.* 1977)

Loring *et al.* recently presented a diagrammatic treatment of energy transport on substitutionally disordered lattices (Loring *et al.* 1983 a, b, 1984 a). This approach is analogous to the GAF treatment (Gochanour *et al.* 1979) of the continuum energy transport problem. The lattice problem is complicated by the fact that a lattice site can be occupied by at most one chromophore. Therefore the chromophore positions are correlated and ensemble averages must be taken only over allowed configurations. This makes the lattice problem much more difficult from a theoretical perspective (Sakun 1973, Korzeniewski *et al.* 1983).

In order to illustrate some distinctive features of energy transport on a lattice, we examine results for the case in which the transfer rate is non-zero only between

chromophores that are nearest neighbours on the lattice. This problem has a percolation threshold. Below some critical concentration, the chromophores exist only in clusters of finite size. The mean-square displacement cannot grow linearly at long times and $\hat{D}(0,0)$, the long-time limit of the diffusion constant, should be zero. Curve *N* in figure 10 illustrates the behaviour of $\hat{D}(0,0)$ for a nearest-neighbour rate of magnitude *w* on a simple cubic lattice of spacing *a*. $\hat{D}(0,0)$ has the exactly correct value at $c=1$, approaches zero as *c* approaches 0·346 from above, and is zero below this concentration (*c* is the fraction of sites occupied by donor chromophores). The critical concentration for site percolation on a simple cubic lattice has been calculated by Monte Carlo methods to be approximately 0·312 (Kirkpatrick 1976). Thus the calculated $\hat{D}(0,0)$ has a physically reasonable concentration dependence.

For any transfer rate of infinite range, however rapidly decaying with distance, such as that resulting from multipolar or exchange interactions, percolation effects will be absent. Curve F in figure 10 illustrates the concentration dependence of $\hat{D}(0,0)$ for an orientationally averaged Förster dipole–dipole transfer rate on a simple cubic lattice. The result for $c=1$ is the exact result for an ordered lattice given by Förster (1948). The dashed curve shows $\hat{D}(0,0)$ of GAF for a continuum. Figure 10 shows that for small *c*, the lattice $\hat{D}(0,0)$ approaches the continuum result of GAF (Gochanour *et al.* 1979). We expect that in the limit of low concentration, the discrete nature of the lattice will cease to be important and that transport on a disordered lattice will resemble transport in a



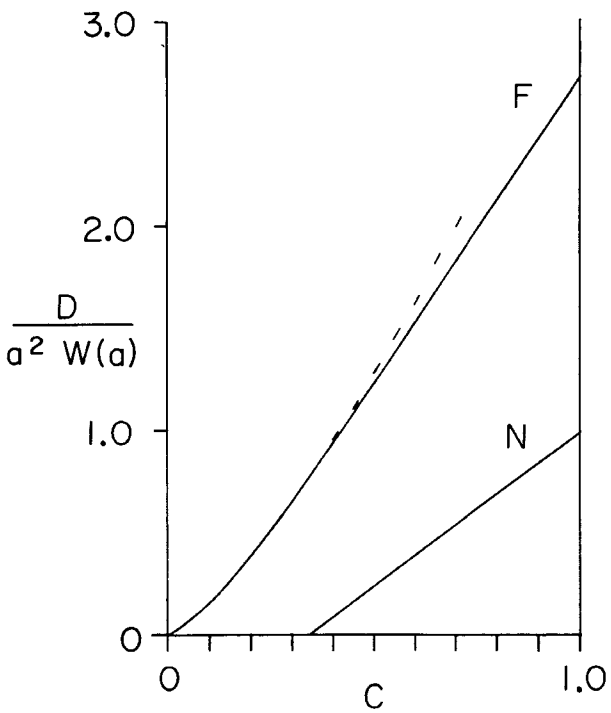


Figure 10. The concentration dependence of the diffusion constant *D* for a nearest-neighbour transfer rate (N) and for a Förster dipole–dipole transfer rate (F) on a simple cubic lattice of spacing *a*. *w*(*a*) is the nearest-neighbour step rate. The dashed curve shows *D* for the Förster rate in a continuum calculated using the GAF theory.

continuum. Thus the lattice $\hat{D}(0,0)$ shown in figure 10 has the exactly correct value at $c=1$, approaches an accurate continuum approximation at low concentration, and hence is expected to be accurate for intermediate concentrations. This is the first theory of hopping transport on a randomly substituted lattice which is not restricted to low concentration that can be applied in the case of a long-range transfer rate.

Time-dependent observables can also be calculated for the lattice problem. We can test the accuracy of the $G^s(t)$ calculation at $c=1$ by examining the case of nearest-neighbour hopping on a filled simple cubic lattice. $G^s(t)$ cannot be calculated exactly in closed form for a filled lattice of arbitrary type and a transfer rate of arbitrary distance dependence. However, for the case of a transfer rate that is non-zero only between nearest neighbours on a filled simple cubic lattice, $G^s(t)$ can be calculated exactly (Barber and Ninham 1970). Figure 11 shows plots of the exact $G^s(t)$ (A) and the approximate $G^s(t)$ (B) for this case. The approximate $G^s(t)$ is practically indistinguishable from the exact answer for a filled lattice. Since the low-concentration limit of the lattice problem approaches the accurate continuum approximation, the calculation of $G^s(t)$ should be accurate for any concentration.

All the calculations illustrated in figures 10 and 11 were performed for a simple cubic lattice. The lattice theory is not restricted to this and can be applied to any lattice type of any dimensionality with any transfer rate. The results are expected to be good approximations over the full range of concentration.



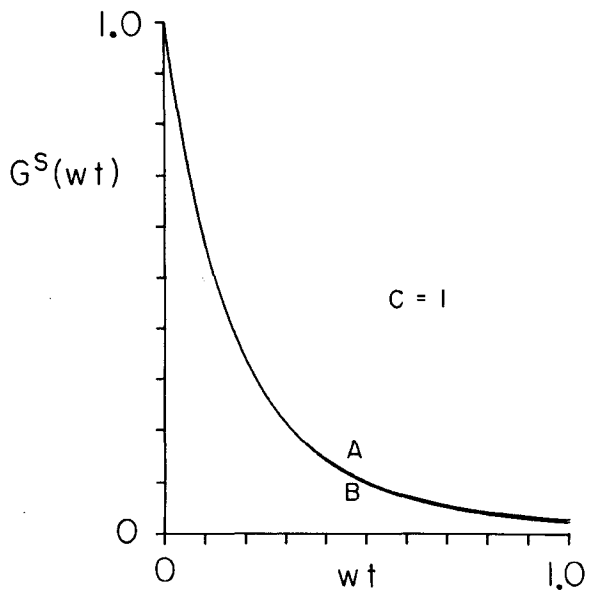


Figure 11. $G^s(wt)$, the probability that an initially excited chromophore retains its excitation after a time $wt$, for a filled simple cubic lattice and a nearest-neighbour transfer rate. Curve A is the exact result, and curve B is the approximate result calculated with the LAF lattice theory. The approximation is seen to be highly accurate for this case. The LAF lattice theory gives an accurate description of transport on a lattice for any distance dependence of the transfer rate, for any lattice type, and for any concentration from a filled to an empty lattice.

### 5.2. *Trapping observables*

The theory discussed above can be extended to include trapping on a lattice with two types of chromophore. The approximation developed for this case is valid for any donor concentration but for only low trap concentration. (Loring *et al.* 1984 b). This modification makes the previous theory applicable to a larger group of experiments. Transport in the presence of traps is intrinsically interesting and must be understood for the practical reason that low-concentration traps are necessarily present in crystals of all types. For example, chemical (Gentry and Kopelman 1983, Gentry 1983, Kopelman 1981, Smith *et al.* 1977, Colson *et al.* 1977) and defect (Blott *et al.* 1978) traps have been studied in molecular crystals, and chromium dimer traps have been studied in ruby (Imbush 1967).

Transport and trapping of excited states have been studied in a variety of mixed molecular crystals using steady-state optical experiments. (Gentry and Kopelman 1983, Gentry 1983, Kopelman 1981, Smith *et al.* 1977, Colson *et al.* 1977). It is generally found that for low trap concentration the fraction of luminescence from the traps is strongly dependent on donor concentration. For low donor concentrations, the relative trap luminescence increases slowly with increasing donor concentration until a characteristic concentration is reached at which trapping becomes very efficient and a substantial fraction of the total luminescence comes from the traps. This effect is easy to interpret qualitatively for a system in which the trap concentration is low and interactions are of short range, so that most trapping events are preceded by a series of donor–donor hops. At low donor concentrations, most excitations will be restricted to small clusters of donors and little trapping will occur. As the donor concentration is raised, a concentration will be reached at which the donor system is sufficiently connected that paths of interacting donors will lead to most traps, and most of the excitations will be trapped. Thus, measurements of the relative trap luminescence at fixed low trap concentration as a function of donor concentration will yield information about the extent of donor–donor transport in the system.



$I(c_D, c_T)$, the integrated trap luminescence normalized by the sum of the integrated luminescence from donors and traps, can be calculated in a straightforward way from the Green function for the transport problem. Here $c_D$ and $c_T$ are the fraction of sites occupied by donors and traps, respectively. Since $I(c_D, c_T)$ is a steady-state observable it can be calculated directly from the Laplace transform of the Green function, eliminating the need for numerical Laplace inversion.

Figure 12 shows a comparison between the continuum trapping theory of Section 3 (Loring *et al.* 1982 a, b, Loring and Fayer 1982) and the lattice theory. Let $w(r)$ and $v(r)$ be the donor-donor and donor–trap transfer rates, respectively, while $a/R$ is the ratio of the lattice spacing to the interaction length. Curve L in figure 12 (*a*) shows $I(c_D, c_T)$ for a square lattice, $c_T = 10^{-3}$, $w(r) = v(r) = \tau_D^{-1}(R/r)^{14}$, $a/R = 0{\cdot}6$, and curve L in figure 12 (*b*) shows $I(c_D, c_T)$ for the same system with $a/R = 0{\cdot}4$. The curve labelled C in each figure is a calculation from the continuum theory with the same number densities of donors and traps. The two theories agree at small values of $c_D$ and this agreement improves as the interaction length $R$ becomes large relative to the lattice spacing. Figure 12 (*c*) shows the same calculations as figure 12 (*a*) and (*b*) with transfer rates $w(r) = v(r) = \tau_D^{-1}(R/r)^6$. (Note that for a given value of $a/R$, $w(a)$ will be much larger for the transfer rate of figure 12 (*a*) and (*b*) than for the transfer rate of figure 12 (*c*). The discrepancies between the lattice and continuum results can be large even for this longer-ranged transfer rate. These figures indicate that the application of a continuum theory to experiments on mixed crystals may be inappropriate unless the interaction length is very large relative to lattice parameters.

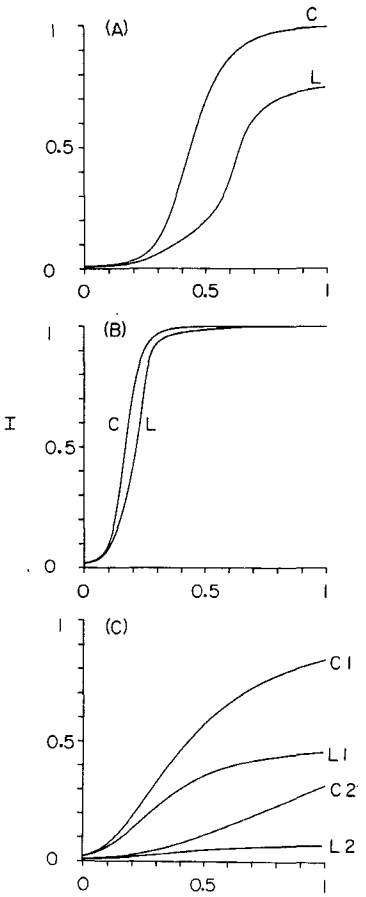


Figure 12. Comparison of $I(c_D, c_T)$, the integrated trap fluorescence normalized to the sum of the trap and donor fluorescence, for the lattice (L) and the continuum (C) for a square lattice of spacing $a$. (*a*) $c_T = 10^{-3}$; $w(r) = v(r) = \tau_D^{-1}(R/r)^{14}$; $a/R = 0{\cdot}6$. (*b*) $c_T = 10^{-3}$; $w(r) = v(r) = \tau_D^{-1}(R/r)^{14}$; $a/R = 0{\cdot}4$. (*c*) Curves C1 and L1 have the same parameters as (*b*) but with $w(r) = v(r) = \tau_D^{-1}(R/r)^6$. Curves C2 and L2 have the same parameters as (*a*) but with $w(r) = v(r) = \tau_D^{-1}(R/r)^6$. The continuum and lattice theories agree only for very low $c_D$ and small $a/R$.

Singlet and triplet energy transport and trapping in an effectively two-dimensional system (perdeuteronaphthalene/naphthalene/betamethylnaphthalene mixed crystals) has been extensively studied by Kopelman and co-workers (Gentry and Kopelman 1983, Gentry 1983, Kopelman 1981). In our designation, naphthalene is the donor and betamethylnaphthalene is the trap. Measurements on singlet excitation transport on this system by Gentry and Kopelman (1983) are depicted in figure 13 (circles). $c_T$ could not be kept exactly constant for these measurements, but varies from $3 \times 10^{-4}$ to $1 \times 10^{-3}$. The squares in figure 13 are the result of a lattice calculation of $I(c_D, c_T)$ for a square lattice, $w(r) = v(r) = \tau_D^{-1}(R/r)^{14}$, and $a/R = 0{\cdot}6$. We have chosen an orientationally averaged octupole–octupole transfer rate because the transition dipole of naphthalene is known to be small and cannot account for the pure naphthalene crystal exciton band structure (Craig and Walmsley 1968). The octupole–octupole term is the next

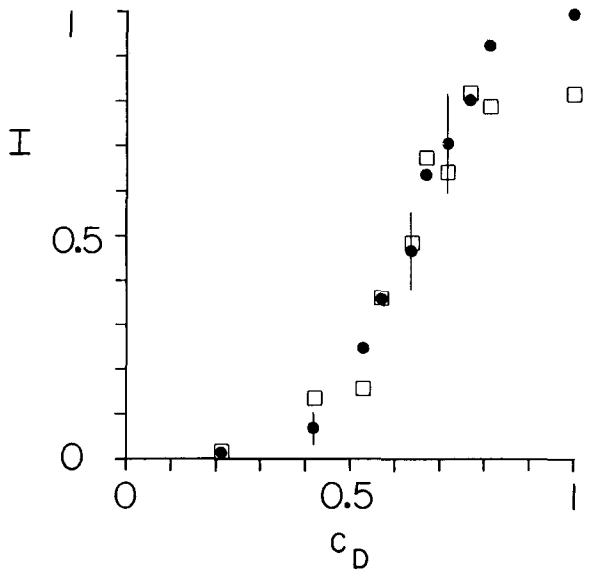


Figure 13. The filled circles are measurements of singlet excitation transport, $I(c_D, c_T)$, in mixed naphthalene crystals at 4·2 K by Gentry and Kopelman (1983). The squares are calculated for a square lattice with the $c_T$ values given by Gentry and Kopelman. $a/R = 0{\cdot}60$ and $w(r) = v(r) = \tau_D^{-1}(R/r)^{14}$. The calculated points do not lie on a smooth curve because of the variation in $c_T$, which ranges from $3 \times 10^{-4}$ to $1 \times 10^{-3}$.



symmetry allowed term in a multipolar expansion of the intermolecular interaction (Craig and Walmsley 1968). The calculated points do not lie on a smooth curve as in figure 12 because of the variation in trap concentration. The error bars on the data increase with increasing $I(c_D, c_T)$ because of difficulties in extracting the naphthalene fluorescence from the betamethylnaphthalene phonon sideband, which overlaps it (Gentry and Kopelman 1983, Gentry 1983). The error bars on the three points at highest concentration are larger than the error bar on the point at $c_D = 0{\cdot}72$ (R. Kopelman, personal communication). Within the experimental uncertainty, the calculated results and the data are in good agreement.

The agreement between the calculation and the data should not be interpreted as a proof that an incoherent hopping model is a valid description of energy transfer in naphthalene at 4·2 K. It is conceivable that the model applies for low donor concentration (strong spatial disorder) but that transfer is partially coherent at high donor concentration. The fact that a master equation approach may be least applicable at high $c_D$ for low-temperature experiments may account for the discrepancy between data and calculation for the two points with highest $c_D$ in figure 13. The resolution of questions concerning the nature of energy transfer in mixed molecular crystals at low temperature must await theories that take into account incoherent phonon-assisted hopping among molecules with different site energies and the possibility of partially coherent transfer. The theory discussed briefly in this section will be applicable without ambiguity to energy and charge-carrier transfer in mixed crystals at higher temperatures where an incoherent hopping model is known to be valid.

## 6. Concluding remarks

In this paper we have discussed recent developments in the field of excitation transport in disordered systems. While we presented the theoretical aspects of this subject in terms of excitation transport, the methods described here also apply to electron transport in disordered crystals or amorphous materials. For these systems, experimental observables such as the a.c. conductivity can be calculated from the diagrammatic theories of transport.

In another paper (Ediger and Fayer 1984) recent progress is discussed in the study of finite-volume, excitation-transport systems. These systems are characterized by chromophore distributions which are not spatially homogeneous at microscopic dimensions. The combination of an accurate theory and careful experiments can provide information about the spatial extent of chromophore distributions, e.g., the average radius of gyration of an isolated polymer coil in a polymer blend (Ediger *et al.* 1985).

The advances discussed in this article have been both theoretical and experimental. The combination of new time-resolved experimental techniques with an increasingly sophisticated approach to the complex statistical mechanical problem has increased our depth and range of understanding. The excitation-transport process is not generally diffusive. For systems involving a random distribution of intermolecular distances, excitation transport and trapping cannot be described by simple rate constants. This can have important implications. For example, in photochemistry, complex reaction schemes involving energy transfer generally employ energy-transfer rate constants which should actually be time-dependent rate functions.

The work described here addressed the incoherent transport of excitations in disordered systems. For many situations we have a quite complete understanding of transport processes. However, there are a great number of important questions which remain unanswered. For example, on what time scale is a master equation the proper description of the system? The master equation describes the flow of probabilities according to classical mechanics. On a fast enough time scale, quantum mechanical probability amplitudes, rather than probabilities, must come into play. In a highly concentrated system, is the initial condition a delocalized state which rapidly damps into a localized incohereht excitation? If so, how fast does the damping take place? The master equation applies on a time scale that is long compared with this. Questions such as these, and problems involving the temperature dependence of transport in disordered systems and the role played by energy inhomogeneity, combine to form a related set of fundamental problems which remain unanswered.



## Acknowledgments

The work described here involved the efforts of a number of individuals at Stanford over the course of several years and we would like to take this opportunity to acknowledge them. Professor Hans C. Andersen, Dr. C. R. Gochanour and Roger F. Loring were involved in various aspects of the development and application of the diagrammatic, nonperturbative excitation transport theory. Dr. C. R. Gochanour, Professor R. J. Dwayne Miller and Dr. Marc Pierre were responsible for the picosecond experiments on transport and trapping in solution. Dr. D. R. Lutz, Professor Keith A. Nelson and Dr. C. R. Gochanour were involved in the experiments on fluorescence quenching in concentrated dye solutions.

This work was made possible by substantial financial support from the National Science Foundation, Division of Materials Research (Grant No. DMR 84-16343) and

by the Department of Energy, Office of Basic Energy Sciences (No. DE-FG03-84ER13251). In addition, the National Science Foundation Stanford Center for Materials Research contributed to the support of this research. MDF would like to acknowledge the Simon Guggenheim Memorial Foundation for Fellowship support which contributed to this research.

## References

ANDERSON, R. A., REED, R. F., and SOUTAR, I., 1980, *Eur. Polym. J.*, **16,** 945.
BARBER, M. A., and NINHAM, B. W., 1970, *Random and Restricted Walks* (New York: Gordon & Breach).
BEDDARD, G. S., and PORTER, G., 1976, *Nature*, **260,** 366.
BERLMAN, I., 1973, *Energy Transfer Parameters of Aromatic Molecules* (New York: Academic), pp. 27–47, and references therin.
BIRKS, J. B., 1970, *Photophysics of Aromatic Molecules* (New York: Wiley-Interscience), pp. 142–92.
BOJARSKI, C., KUŚBA, J., and OBERMULLER, G., 1975, *Acta Phys. Polon.* A, **48,** 85.
BURLAND, D. M., KONZELMANN, V., and MACFARLANE, R. M., 1977 a, *J. Chem. Phys.*, **67,** 1926.
BURLAND, D. M., COOPER, D. E., FAYER, M. D., and GOCHANOUR, C. R., 1977 b, *Chem. Phys. Lett.*, **52,** 279.
CHUANG, T. J., and EISENTHAL, K. B., 1971, *Chem. Phys. Lett.*, **11,** 368.
COLSON, S. D., GEORGE, S. M., KEYES, T., and VAIDA, V., 1977, *J. chem. Phys.*, **67,** 4941.
CRAIG, D. P., and WALMSLEY, S. H., 1968, *Excitons in Molecular Crystals* (New York: Benajamin), p. 107.
CRAVER, F. W., and KNOX, R. S., 1971, *Molec. Phys.*, **22,** 385 and references therein.
DALE, R. E., and EISINGER, J., 1976, *Proc. natn. Acad. Sci. U.S.A.*, **73,** 271.
DAVYDOV, A. S., 1971, *Theory of Molecular Excitons* (New York: Plenum).
DEXTER, D. L., 1953, *J. chem. Phys.*, **21,** 836.
DLOTT, D. D., FAYER, M. D., and WIETING, R. D., 1978, *J. chem. Phys.*, **69,** 2752.
EDIGER, M. D., DOMINGUE, R. P., and FAYER, M. D., 1984, *J. chem. Phys.*, **80,** 1246.
EDIGER, M. D., DOMINGUE, R. P., PETERSON, K. A., and FAYER, M. D., 1985, *Macromolecules*, **18,** 1182.
EDIGER, M. D., and FAYER, M. D., 1983, *Macromolecules*, **16,** 1839.
EDIGER, M. D., and FAYER, M. D., 1984, *J. phys. Chem.*, **88,** 6108.
FAYER, M. D., 1982, *Ann. Rev. phys. Chem.*, **33,** 63.
FÖRSTER, TH., 1948, *Ann. Phys. Leipzig*, **2,** 55.
FÖRSTER, TH., 1949, *Z. Naturf.* (a), **4,** 321.
FRANK, C. W., GASHGARI, M.-A., CHUTIKAMONTHAM, P., and HAVERLY, V. J., 1980, *Studies in Physical and Theoretical Chemistry*, Vol. 10, edited by A. G. Walton (Amsterdam: Elsevier), pp. 187–209.
FRANK, C. W., and HARRAH, L. A., 1974, *J. Chem. Phys.*, **61,** 1526.
FREDRICKSON, G. H., ANDERSEN, H. C., and FRANK, C. W., 1983 a, *Macromolecules*, **16,** 1456.
FREDRICKSON, G. H., ANDERSEN, H. C., and FRANK, C. W., 1983 b, *J. chem. Phys.*, **79,** 3572.
FREDERICKSON, G. H., ANDERSEN, H. C., and FRANK, C. W., 1984, *Macromolecules*, **17,** 1496.
GALANIN, M. D., 1950, *Tr. Fiz. Inst. I. P. Pavlova*, **5,** 341.
GELLES, R., and FRANK, C. W., 1982, *Macromolecules*, **15,** 1486.
GENTRY, S. T., 1983, Ph.D. Thesis, University of Michigan, Ann Arbor, Michigan.
GENTRY, S. T., and KOPELMAN, R., 1983, *J. chem. Phys.*, **78,** 373.
GOCHANOUR, C. R., ANDERSEN, H. C., and FAYER, M. D., 1979, *J. chem. Phys.*, **70,** 4254.
GOCHANOUR, C. R., and FAYER, M. D., 1981, *J. phys. Chem.*, **85,** 1989.
GROVER, M., and SILBEY, R., 1970, *J. chem. Phys.*, **52,** 2099.
GROVER, M., and SILBEY, R., 1974, *J. chem. Phys.*, **54,** 4943.
HAAN, S. W., and ZWANZIG, R., 1978, *J. chem. Phys.*, **68,** 1879.
HAAS, E., WILCHEK, M., KATACHALSKI-KATZIR, E., and STEINBERG, I. Z., 1975, *Proc. natn. Acad. Sci., U.S.A.*, **72,** 1807.
HEMENGER, R. P., and PEARLSTEIN, R. M., 1973, *J. chem. Phys.*, **59,** 4064.
HETHERINGTON, W. M., MICHAELS, R. H., and EISENTHAL, K. B., 1979, *Chem. Phys. Lett.*, **66,** 230.

IMBUSCH, G. F., 1967, *Phys. Rev.*, **153,** 326.
INOKUTI, M., and HIRAYAMA, F., 1965, *J. chem. Phys.*, **43,** 1978.
JABLOŃSKI, A., 1970, *Acta Phys. Polonica* A, **38,** 453.
KENKRE, V. M., and KNOX, R. S., 1974 a, *Phys. Rev.* B, **9,** 5279.
KENKRE, V. M., and KNOX, R. S., 1974 b, *Phys. Rev. Lett.*, **33,** 804.
KENNEY-WALLACE, G. A., FLINT, J. H., and WALLACE, S. C., 1975, *Chem. Phys. Lett.*, **32,** 71.
KIRKPATRICK, S., 1976, *Phys. Rev. Lett.*, **36,** 69.
KLAFTER, J., and JORTNER, J., 1977, *Chem. Phys. Lett.*, **49,** 410.
KLÖPFFER, W., 1981, *Ann. N. Y. Acad. Sci.*, **366,** 373.
KOGLIN, K. F., MILLER, J., STEINWANDEL, J., and HAUSER, M., 1981, *J. phys. Chem.*, **85,** 2363.
KOPELMAN, R., 1981, *Topics in Applied Physics*, Vol. 49, edited by W. M. Yen and P. M. Seltzer (Berlin: Springer), p. 241.
KORZENIEWSKI, G., FRIESNER, R., and SILBEY, R., 1983, *J. statist. Phys.*, **31,** 451.
LORING, R. F., ANDERSEN, H. C., and FAYER, M. D., 1982 a, *J. chem. Phys.*, **76,** 2015.
LORING, R. F., ANDERSEN, H. C., and FAYER, M. D., 1982 b, *J. chem. Phys.*, **77,** 1079(E).
LORING, R. F., ANDERSEN, H. C., and FAYER, M. D., 1983 a, *Phys. Rev. Lett.*, **50,** 1324.
LORING, R. F., ANDERSEN, H. C., and FAYER, M. D., 1983 b, *Phys. Rev. Lett.*, **51,** 718(E).
LORING, R. F., ANDERSEN, H. C., and FAYER, M. D., 1984 a, *J. chem. Phys.*, **80,** 5731.
LORING, R. F., ANDERSEN, H. C., and FAYER, M. D., 1984 b, *Chem. Phys.*, **85,** 149.
LORING, R. F., and FAYER, M. D., 1982, *Chem. Phys.*, **70,** 139.
LUTZ, D. R., NELSON, K. A., GOCHANOUR, C. R., and FAYER, M. D., 1981, *Chem. Phys.*, **58,** 325.
MARKVART, T., 1978, *J. theor. Biol.*, **72,** 91.
MILLAR, D. P., ROBBINS, R. J., and ZEWAIL, A. H., 1981, *J. chem. Phys.*, **75,** 3649.
MILLER, R. J. D., PIERRE, M., and FAYER, M. D., 1983, *J. chem. Phys.*, **78,** 5138.
MONTROLL, E. W., 1964, *Proc. Symp. Appl. Math.* (Am. Math. Soc., Providence, R.I.) **16,** 193.
MOOG, R. S., EDIGER, M. D., BOXER, S. G., and FAYER, M. D., 1982, *J. phys. Chem.*, **86,** 4694.
MOOG, R. S., KUKI, A., FAYER, M. D., and BOXER, S. G., 1984, *Biochemistry*, **23,** 1564.
NELSON. K. A., MILLER, R. J. D., LUTZ, D. R., and FAYER, M. D., 1982, *J. appl. Phys.*, **53,** 1144.
NG, D., and GUILLET, J. E., 1982, *Macromolecules*, **15,** 728.
PARSON, R., 1983, *Chem. Phys. Lett.*, **99,** 213.
PEARLSTEIN, R. M., 1964, *Proc. natn. Acad. Sci., U.S.A.*, **52,** 824.
PORTER, G., 1978, *Proc. R. Soc.* A, **362,** 281.
PORTER, G., SADKOWSKI, P. J., and TREDWELL, C. J., 1977, *Chem. Phys. Lett.*, **49,** 416.
PORTER, G., and TREDWELL, C. J., 1978, *Chem. Phys. Lett.*, **56,** 278.
REHM, D., and EISENTHAL, K. B., 1971, *Chem. Phys. Lett.*, **9,** 387 and references therein.
ROSE, S., RIGHINI, R., and FAYER, M. D., 1984, *Chem. Phys. Lett.*, **106,** 13.
SAKUN, V., 1973, *Soviet Phys. solid St.*, **14,** 1906.
SAUER, K., 1978, *Accts Chem. Res.*, **7,** 257.
SCHÄFER, F. P., 1971, *Topics in Applied Physics*, second edition, edited by F. P. Schäfer (New York: Springer-Verlag), **1,** 21–24, 158–60.
SCHER, H., ALEXANDER, S., and MONTROLL, E. W., 1980, *Proc. natn. Acad. Sci., U.S.A.*, **77,** 3758.
SELWYN, J. E., and STEINFELD, J. I., 1972, *J. phys. Chem.*, **76,** 762.
SELZER, P. M., HAMILTON, D. S., and YEN, W. M., 1977, *Phys. Rev. Lett.*, **38,** 858.
SMITH, D. D., MEAD, R. D., and ZEWAIL, A. H., 1977, *Chem. Phys. Lett.*, **50,** 358.
STEHFEST, H., 1970, *Commun. Assoc. Comput. Mach.*, **13,** 47, 624.
VAVILOV, S. I., and GALANIN, M. D., 1949, *Soviet Phys. Dokl.*, **67,** 811.
WIETING, R. D., FAYER, M. D., and DLOTT, D. D., 1978, *J. chem. Phys.*, **69,** 1996.